J Mater Sci: Mater Electron (2018) 29:1504–1509
DOI 10.1007/s10854-017-8059-z

Nonlinear optical absorption studies of $CoMoO_4$ hybrid nanostructures

K. Mani Rahulan[1] · **N. Angeline Little Flower**[1] · **R. Annie Sujatha**[1] ·
N. Padmanathan[2] · **C. Gopalakrishnan**[3]

Received: 5 August 2017 / Accepted: 14 October 2017 / Published online: 20 October 2017
© Springer Science+Business Media, LLC 2017

Abstract The present work aims at the synthesis of $CoMoO_4$ hybrid nanorods by hydrothermal method. The optical and structural properties of the synthesized nanorods have been characterized by X-ray diffraction (XRD), Fourier transform infrared spectroscopy (FTIR) and Scanning electron microscopy (SEM). Nonlinear optical studies of the samples were measured by single-beam open aperture Z-scan technique using 5 ns laser pulses at 532 nm. The measured optical nonlinearity of the nanorods shows a typical third order nonlinear optical behaviour including two-photon absorption (2 PA) and reverse saturable absorption (RSA). Experimental findings show that the presence of RSA in these nanoparticles makes them a promising candidate for the fabrication of optical limiting devices.

1 Introduction

The search for efficient materials in the field of non-linear optics has been a very remarkable field of research for several years [1–3]. Applications of lasers and laser based devices have become more common in our daily life and it is well recognized that high intensity laser beams cause hazards to delicate optical components especially the human's eyes. Thus, Protection of optical components from powerful lasers is one of the greatest concerns in the modern opto-electronic era and this has led to the study and development of optical limiting materials. Transition metal oxides, such as Co_3O_4, V_2O_5 and CuO have been intensively investigated over the past few decades, because of their large optical nonlinearity and the advantages of good thermal and chemical stability in addition to mechanical strength [4–6]. On the other hand, allotropes of carbon have shown interesting nonlinear optical (NLO) properties and contribute a lot to optical limiting applications. Carbon black suspensions, carbon nanoparticles, fullerenes, and carbon nanotubes exhibit a remarkable nonlinear extinction effect with intense laser beams. In recent years, graphene, a two-dimensional nano-carbon system, has provided a breakthrough in materials science because of its excellent mechanical, electrical and optical properties owing to its unique structure. A number of reports on the nonlinear optical response of graphene have been studied extensively by many researchers [7–12]. Graphene based materials like exfoliated graphite, graphene oxide (GO), and reduced GO (rGO) are promising materials because it is relatively easy to process and functionalize them. Integration of graphene with other hybrid materials can significantly enhance the NLO and optical limiting properties owing to donor acceptor system. For instance, the optical limiting properties of cobalt and carbon nanotubes were reported by few researchers [13–15].

The present work being among the few existing experimental investigations regarding the NLO response of $CoMoO_4$ hybrid nanostructure systems, aims to study the optical limiting behavior using z-scan technique. To investigate the optical limiting mechanism present in these nanostructures, the measured experimental data is numerically modeled to the appropriate nonlinear transmission equations. Based on the measured data and the numerically calculated values of the nonlinear optical parameters, we demonstrate

---

✉ K. Mani Rahulan
krahul.au@gmail.com

[1] Department of Physics and Nanotechnology, SRM University, Chennai 603203, India

[2] Tyndall National Institute, University College Cork, Cork, Ireland

[3] Nanotechnology Research Center, SRM University, Kattankulathur, Chennai 603203, India

that two-photon absorption (2 PA) in nanosecond regime are responsible for the nonlinear optical absorption (NLA) behavior observed in these materials.

2 Experimental technique

2.1 Cobalt molybdate carbon

The $CoMoO_4$ nanostructures were synthesized by a simple hydrothermal approach using sodium molybdate and cobalt nitrate as the starting precursors. All the reagents are analytical grade purchased from Alfa Aesar and used as received without further purification. For $CoMoO_4$/C hybrid nanostructure, the stoichiometric amount of $Co(NO_3)_2{\cdot}6H_2O$ and $Na_2MoO_4{\cdot}2H_2O$ were dissolved in 40 ml deionized (DI) water under stirring. After stirring of about 10 min, 1 g of D-glucose solution was added to the above mixed solution and continued stirring for 30 min.

Obtained violet colour precipitated solution was transferred to Teflon-lined stainless steel autoclave and kept in oven at 180 °C for 12 h. Finally, it was cooled down to room temperature naturally and the precipitate was separated, washed with deionized (DI) water, ethanol and acetone consecutively. Finally, the end product was dried at room temperature followed by the calcination at 450 °C under argon for 2 h.

2.2 Cobalt molybdate pure

Similarly, the pristine $CoMoO_4$ also synthesized without adding D-glucose under the same experimental conditions mentioned above.

2.3 Cobalt molybdate graphene

In order to fabricate $CoMoO_4$/rGO nanorods, first graphite oxide (GO) was synthesized from graphite flakes by modified Hummers method as reported earlier [16]. Simply, 1 g of graphite flakes was dispersed in 50 ml of fumic sulfuric acid under stirring at 0 C. After that, the 0.5 g of $NaNO_3$ and excess amount of potassium permanganate was added the brown color precipitate was immediately formed. In continuation, the 200 ml deionized water followed by 30% H_2O_2 (8 ml) was added under vigorous stirring.

Finally, the yellow color GO solution was obtained and washed with HCL aqueous solution followed by excess amount of water several times until to neutral pH. As prepared dark brown GO (10%) was dispersed in 40 ml deionized water by ultrasonication. Pre-prepared $Co(NO_3)_2{\cdot}6H_2O$ and $Na_2MoO_4{\cdot}2H_2O$ suspension was added to GO solution and stirred for 30 min. The mixed solution was transmitted to a Teflon-lined stainless steel autoclave and kept at 180 °C for 12 h. After cooling down to room temperature naturally, the precipitate was separated by centrifugation. After washed with DI water, ethanol and acetone several times, the end product was dried at room temperature and heat treated under Ar atmosphere for 2 h at 450 °C in the heating rate of 5° min^{-1}.

2.4 NLO properties measurements

Optical limiting properties were investigated from open aperture Z-scan experiments with 5 ns laser pulses at 532 nm from a frequency doubled, Q switched Nd:YAG laser (Minilite Continuum Inc.). Samples were prepared by dispersing the nanoparticles in ethylene glycol and the solution was taken in a 1 mm cuvette. The samples were adjusted to have the linear transmittance of 65%. The spatial profile of the pulsed beam was of nearly Gaussian form after spatial filtering. The pulsed beam was split into two parts by a beam splitter: the transmitted part was focused onto samples by using a 20-cm focal length lens and the reflected part was used as reference. At each position z, the sample experienced different laser intensity, and the position dependent (i.e., intensity-dependent) transmission was measured using an energy meter placed after the sample. Laser pulses were excited at a repetition rate of 1 Hz, and the data acquisition was automated. The low repetition rate was chosen for avoiding thermal effects in the samples during measurement. The pulse energy reaching the sample was approximately 150 mJ.

3 Results and discussion

3.1 X-ray diffraction

The powder XRD patterns of the hydrothermally synthesized pristine and hybrid $CoMoO_4$ nanostructures are shown in Fig. 1. The diffraction peaks of the samples can be ascribed to cobalt molybdate and are well matched in concordance with the standard JCPDS (26-0477) card. No peaks due to impurities or other residuals was observed for pure cobalt molybdate, indicating the high purity of the hydrothermally synthesized $CoMoO_4$ nanostructures. Further, the crystallinity of the hybrid cobalt molybdate carbon was comparatively higher than the pure cobalt molybdate. The broad and weak diffraction peaks pattern evidenced small crystallite size and poor crystallization nature of the samples.

3.2 Scanning electron microscopy

The surface morphology and microstructure of the $CoMoO_4$ hybrid nanostructure were investigated by scanning electron microscope. The pictures clearly depict that the product consist of large number of well segregated distinct nanorods.

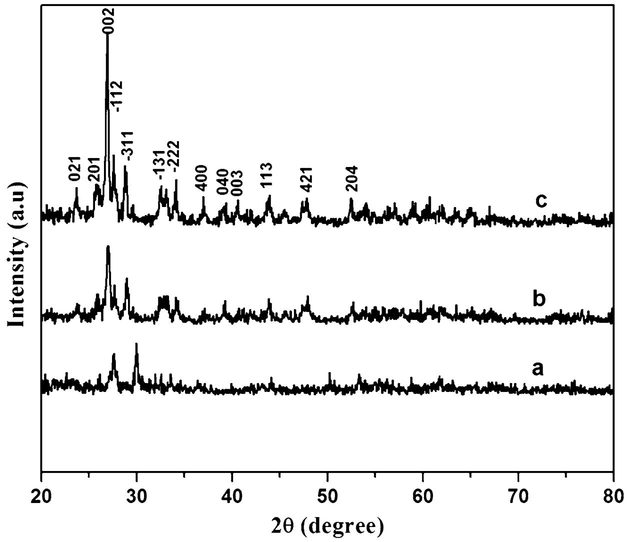

Fig. 1 XRD pattern of (*a*) pure $CoMoO_4$, (*b*) $CoMoO_4$/carbon, (*c*) $CoMoO_4$/graphene

Typical diameter of the nanorods is in the range of 30–60 nm and 1–3 μm in length for all the three $CoMoO_4$ nanostructures. Pure $CoMoO_4$ composites show uniform growth of the nanorods as shown in Fig. 2a. For $CoMoO_4$ /carbon composites, the SEM image has shown the well-distributed nanorods of uniform length as illustrated in Fig. 2b. Similarly incorporation of graphene on $CoMoO_4$ had no remarkable influence on the morphology as shown in Fig. 2c.

3.3 Fourier transform infrared (FTIR) spectroscopy

The FTIR specra of pure and hybrid $CoMoO_4$ nanostructures are shown in Fig. 3. It is believed that the absorption peak at 3441 cm^{-1} is attributed to the O–H stretching vibration and its corresponding O–H bending vibration occurs at 1636 cm^{-1}, due to the chemically adsorbed water molecules. For pure $CoMoO_4$, the peak around 866.37 cm^{-1} is due to stretching vibrations of Mo–O–Mo. The vibration band at around 947 cm^{-1} is attributed to the activation of υ_1 vibration of the distorted MoO_4 tetrahedral present in $CoMoO_4$.

Fig. 2 SEM picture of **a** pure $CoMoO_4$, **b** $CoMoO_4$/carbon, **c** $CoMoO_4$/graphene

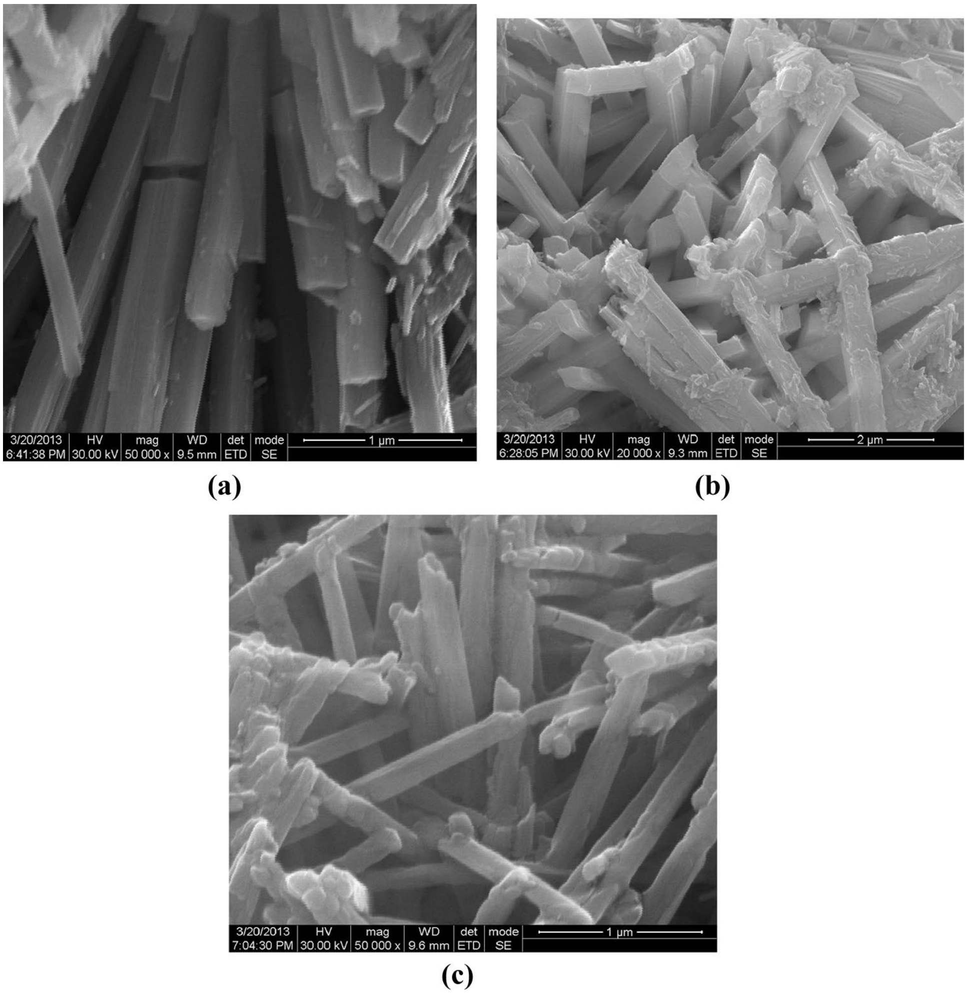
3/20/2013 6:41:38 PM HV 30.00 kV mag 50 000 x WD 9.5 mm det ETD mode SE
1 μm
3/20/2013 6:28:05 PM HV 30.00 kV mag 20 000 x WD 9.3 mm det ETD mode SE
2 μm
3/20/2013 7:04:30 PM HV 30.00 kV mag 50 000 x WD 9.6 mm det ETD mode SE
1 μm

(a)

(b)

(c)

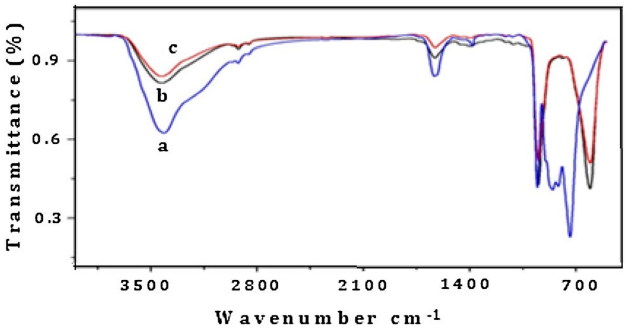

Fig. 3 FTIR spectra of (*a*) $CoMoO_4$, (*b*) $CoMoO_4$/carbon, (*c*) $CoMoO_4$/graphene

The absorption peak at 738 cm^{-1} is assigned to υ_3 vibration of the same group [17].

4 Non linear optical measurements

Open aperture z-scan measurements were performed on cobalt molybdate nanorods with the intention of calculating their nonlinear absorption coefficients. The open aperture Z-scan curves of the samples show a symmetric valley in the normalized transmittance about the focal point (z = 0). The transmissions decrease as the samples move into the beam focus as shown in Fig. 4, indicating the presence of induced absorption in these nanoparticles. The depth of the valley in the z-scan curve is a result of direct indication of the non-linear absorption (NLA) behavior. Different mechanisms are responsible for NLA, the normalized transmittance valley in these materials can be mainly due to two mechanisms, reverse saturable absorption (RSA) and two photon absorption (2PA). The decrease in transmission indicates reverse saturable absorption behavior and this is a typical characteristic for the optical limiting phenomena.

In order to identify the NLA mechanism, the obtained experimental Z-scan data were numerically fitted with appropriate pulse propagation equations. It is found that the measured Z-scan data numerically fits to standard nonlinear transmission equations, including reverse saturable absorption and 2PA. The nonlinear absorption coefficient β is estimated by fitting the experimental curve to the normalized transmission condition given by [18].

$$T = (1-R)^2 \exp(-\alpha L)/\sqrt{\pi} q_0 \int_{-\infty}^{+\infty} \ln\left[\sqrt{1+q_0 \exp(-t^2)}\right] dt$$

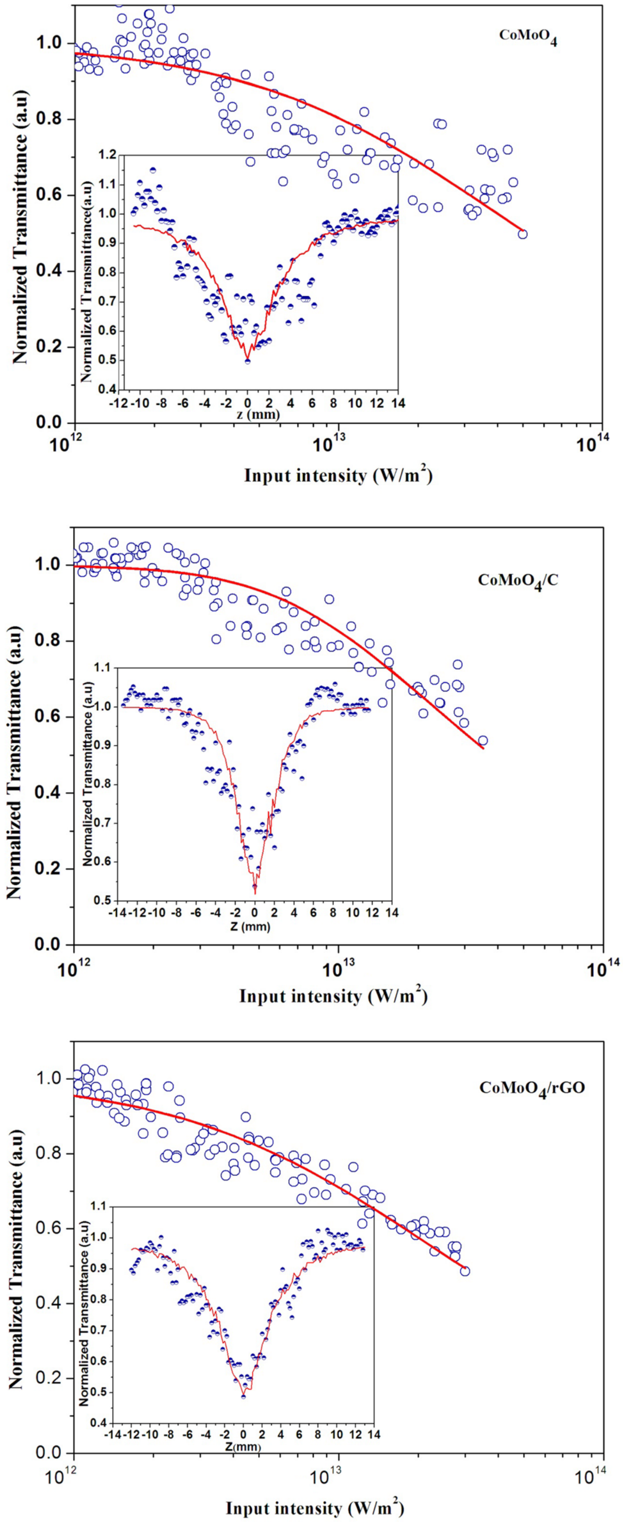

Fig. 4 Normalized transmissions curve of $CoMoO_4$ nanohybrids

where T is the sample transmission given by T(norm) χ linear transmission of the sample, and L and R are the length and surface reflectivity of the sample, respectively. α is the linear absorption coefficient, q_0 is given by β(1 − R) I_0 L_{eff}, where I_0 is the on-axis peak intensity. L_{eff} is given by 1−exp(− αl/α) and β is the effective TPA coefficient.

The solid curve in the figure is the theoretical fit to the experimental data which closely fits well to a two photon absorption 2PA process. Best fits to the data were obtained for a combined process involving RSA and 2PA as the nanostructures were irradiated under ns excitation showing that the nonlinearity is primarily of the third order. This confirms that 2PA is a major mechanism responsible for the optical limiting effect in these nanostructures. It is evident from these optical responses that all the samples revealed a typical optical limiting behavior. The higher the value of β, the better the optical limiting property of the corresponding material. All the three samples have shown greater decreases in normalized transmission at the same pulse intensity at the focus, suggesting that these sample exhibit best optical limiting performance. By fitting the experimental data with the corresponding theoretical equations, the absorption coefficient β for pure $CoMoO_4$, $CoMoO_4$/carbon, and $CoMoO_4$/graphene oxide at 532 nm was calculated to be 1.1×10^{-8}, 6.8×10^{-8} and 8.2×10^{-8} cm W^{-1}, respectively.

The condition for the 2PA process is $Eg > h\nu > Eg/2$. The band gap energy for $CoMoO_4$ nanostructures reported to occur at 2.97 eV [17] is higher than the energy of incident photon (2.33 eV) Eg > hy, the condition for allowed 2PA is satisfied. Therefore, the observed nonlinearity is mainly due to 2PA process. These nanostructures possess relatively large number of defect states within the forbidden energy gap, which may serve as intermediate levels. When these nanostructures are optically pumped at 532 nm (2.3 eV), the electrons can be excited to trapping levels of impurities or crystal defects, which have long lifetimes. These longer lifetimes in intermediate trapping levels result in an enhanced probability for two-step excited state absorption (ESA). It also increases the probability of resonance two-photon transitions. Therefore, the observed nonlinearity can be considered as an “effective” two photon absorption (2PA) process, with contributions from genuine 2PA as well as ESA effects.

It is also worth mentioning that the NLO property has been studied for a new carbon allotropy, graphene, covalently bonded 2D carbon monolayer [19]. Nonlinear optical properties of rGO are related to both sp^2 and sp^3 hybridized domains. Structural defects and oxygen containing functional groups also contribute to the nonlinear optical transmittance and limiting behaviour in rGO. The enhanced nonlinear absorption arises mainly from the defects states due to the functionalization of graphene oxide which facilitate interband transition. Different hybridizations of the carbons and their surface functionalities with cobalt molybdate can give rise to increase nonlinear optical property in the samples. Several parameters should be considered for the enhancement of nonlinear effects such as particle size, surface passivation, nature of organic moieties as well as the electronic band structure of the material.

To check the viability of these hybrid nanostructures as optical limiters, the nonlinear transmission were investigated as a function of input fluence. At low energy fluence the transmission is roughly constant and is below the threshold. When the incident energy exceeds the threshold value, the transmission decreases significantly. It is obvious that, lower the limiting threshold better is the optical limiting material. It can be seen that at higher intensities, all the three composites deviate from the linear transmission. From the measurements, it can be found that composites of these of cobalt molybdate nanostructures are better nonlinear absorbers and hence better optical limiters.

5 Conclusion

In summary, $CoMoO_4$ nanostructures have been synthesized through hydrothermal technique. The results of XRD, SEM and FTIR confirmed the structure and morphology of the synthesized nanostructures. This synthetic procedure be extended to fabricate hybridized $CoMoO_4$/Carbon and $CoMoO_4$/graphene nanostructures. It was found that the diameter of the nanorods lays in the range of 30–60 nm and 1–3 µm in length. Open aperture Z scan measurements performed on this nanostructures exhibits good optical limiting at 532 nm wavelength. All particles display reverse saturable absorption (RSA) at similar intensity in solution. Experimental results show that $CoMoO_4$ and their hybrid structures had an excellent optical limiting property which could be used as a potential candidate to protect from intense laser radiation.

Acknowledgements The authors express their thanks to Dr. Reji Philip of LAMP Group, Raman Research Institute, Bangalore (India) for extending the facilities toward NLO measurements.

References

1. G.S. He, L.S. Tan, Q. Zheng, P.N. Prasad, Chem. Rev. **108**, 1245 (2008)
2. S. Kawata, H.B. Sun, T. Tanaka, K. Tanaka, Nature **412**, 697 (2001)
3. J.W. Perry, *Nonlinear Optics of Organic Molecules and Polymers*. (CRC Press, New York, 1997)
4. X. Zhu, J. Wang, D.T. Nguyen, N. Peyghambarian, Opt. Mater. Express **2**(1), 103–110 (2009)
5. M. Muralikrishna, B.K. Abhijit, P. Prabin, V. Sai Muthukumar, Appl. Phys. A **122**, 757 (2016)
6. H.M. Haider, Y. Muhammad, W. Mahmood, A.I. Yahya, Opt. Quant. Electron **49**:18 (2017)
7. S.R. Sharma, M. Madhuri, K.P. Swapan, J. Phys. Chem. C **119**(21), 12079–12087 (2015)
8. K. Sabira, P. Saheeda, M.C. Divyasree, S. Jayalekshmi, Opt. Laser Technol. **97**, 77–83 (2017)
9. J.L. Cheng, N. Vermeulen, J.E. Sipe, New J. Phys. **16**, 053014 (2014)

10. M. Saravanan, T.C. Sabari Girisun, Appl. Surf. Sci. **392**, 904–911 (2017)
11. P. Prabin, P. Ramakrishna, M. Muralikrishna, K. Adarsh, S. Ramaprabhu, A.M. Rao, V.S. Muthukumar, S.S.S. Sai, Opt. Mater. **39**, 182–187 (2015)
12. Z. Chan, L. Yubing, L. Li Huang, C. Wei, Wenzhe, Opt. Mater. **49**, 152–157 (2015)
13. T.N. Narayanan, C.S. Suchand Sandeep, M.M. Shaijumon, P.M. Ajayan, R. Philip, M.R. Anantharaman, Nanotechnology **20**, 285702–285707 (2009)
14. M. Nadafan, Z. Dehghani, S. ImanFakhrini, Optik-Int. J. Light Electron Opt. **127**(20), 9361–9366 (2016)
15. A. Sousani, H. Motiei, P. Najafimoghadam, R. Hasanzade, Opt. Mater. **67**, 172–179 (2017)
16. N.I. Zaaba., K.L. .Foo, U. Hashim, S.J. Tan, C.H. Voon, Procedia Eng. **184**, 469–477 (2017)
17. R.L. Sutherland, *Handbook of Nonlinear Optics*. (Marcel Dekker, New York, 1996)
18. G. Kianpour, M. Salavati-Niasari, H. Emadi, Superlattices Microstruct. **58**, 120–129 (2013)
19. A.K. Geim, K.S. Novoselov, Nat. Mater. **6**, 183 (2007)